Doubts about the Usefulness of Retina Codes in Biometric Recognition

Thomas Fuhrmann and Andreas Uhl

Department of Computer Sciences, Salzburg University, Austria

{tfuhr,uhl}@cosy.sbg.ac.at

Abstract. We discuss methods for generating retina codes from retinal images for biometric user authentication. First the optical disc as a central reference point is located by using Hough transform followed by a segmentation of the retina vasculature by filtering with the continuous two-dimensional Morlet wavelet transform and classifying each pixel as vessel or non vessel by simple thresholding. Starting from the optical disc, concentric circles are placed over the binary vessel image for data sampling and different variants of retina code are generated after transformation to polar coordinates. The methods inter personal variability and robustness is evaluated on the publicly available DRIVE database. Results indicate a low inter personal variability questioning the usefulness of retina codes in sensible authentication systems. Specifically good robustness against JPEG and JPEG2000 compression is observed.

1 Introduction

With the increasing usage of biometric systems the interest in not-yet widely accepted modalities rises. Retina features are among these potentially promising but not mainstream techniques. Being transparent, the retina is situated in the innermost part of the ocular fundus, retinal features mainly consist of blood vessels originating from the entry point of the optic nerve and spreading across the ocular fundus (see Figs. 1.a and 2.a for examples). The pattern of these vessels is said to be unique for each individual person and might therefore be used for biometric recognition systems. However, the scanning operation is required to be much more intrusive and controlled as compared to e.g. iris-based systems due to the location in the inner parts of the eye and user acceptance of such conditions is generally low. Therefore, the primary application context of this modality will be in high security environments like military or governmental agencies.

According to literature [6, p.106ff], retina-scan based biometric systems exhibit the following strengths:

- Spoofing is difficult
- Usage of a stable physiological trait
- High recognition accuracy

Due to their location at the background of the eye, retinal features can hardly be replaced or modified, also sensors capturing the respective images can hardly by fooled. Therefore, a spoofing attack will be definitively hard to conduct. On the other hand, the stability of retinal vessels is questionable since many eye diseases include some blood vessel pathology as found e.g. in proliferative diabetic retinopathy [7], which is characterized by new vessel growth especially near the optical disk. The possible impact of such diseases on retina feature based biometric systems has to be seriously considered and investigated before a sensible deployment should take place.

Eye-based biometric modalities in general are believed to be highly secure due to the well investigated low FAR of some popular iris recognition systems [8, 9]. However, also in iris recognition several techniques exist which exhibit significantly inferior recognition performance (e.g., based on histograms [10] or wavelet coefficient statistics [11]). As a consequence, it is not only the potential distinctiveness of the physiological trait that determines the recognition accuracy but of course the type of extracted template data plays an at least equally important role as well.

There is not much work available on using retinal features for biometric purposes. Most of the literature on retinal features is found in ophthalmology where retinal vessels are used in diagnosis or as landmarks for image registration (see e.g. [7, 12]). Strengths and weaknesses of retina-scan based biometrics are discussed in [6], but no concrete feature extraction technique or template data structure is described. Crossings of retinal vessels are suggested to be used as biometric features in [13, 14] and good accuracy is reported. Similar to fingerprint minutiae, a type and direction can be associated with each crossing and point pattern matching is performed in the recognition process. Retica Systems Inc.[1] offers a different (commercial) solution based on a "retina code" (inspired by Daugmans' "iris code" principle [8]). Contrasting to the retinal vessels' crossings approach, a reference point is needed to register the images against for this technique.

In this work we discuss the use of retina codes for biometric recognition as inspired by the solution sketched by Retica Systems Inc. In particular, we will address the issue of recognition accuracy for this concrete way to generate template data from retinal features. Section 2 discusses feature extraction techniques for subsequent retina code generation which include optical disc segmentation and retinal vessel extraction. Section 3 describes several variants of retina code generation and Section 4 is devoted to experimental testing with emphasis on the overall code variation within a population (inter person variability is shown to be astonishingly low), FMR under signal distortion, and code sampling. Section 5 concludes the paper.

[1] www.retica.com

2 Feature Extraction Methods

Retina-based methods use ocular fundus images as a source for extracting biometric features for user authentication. Extracting usable feature sets for retina code generation from these images requires a combination of two different preprocessing methods:

1. Finding the Optical Disc as a common reference point
2. Segmenting the retinal vessels

2.1 Optic Disc Segmentation

For retina code generation a reference point has to be defined (analogous to the center of the pupil with iris recognition). Here the optical disc (where the optical nerve leaves the retina) seems suitable. In the retinal images the optical disc appears as a bright circular shaped object partly covered with vessels that has a higher background luminance and higher local variance as the rest of the retina. So the center of the optical disc can be used as a reference point for developing a retina template out of a segmented vessel feature image. However when using an automated method for optical disc location it is important to know that this object varies in appearance, size and location.

Detection of the optical disc has been largely covered in literature and numerous methods have been developed. For our application we first chose a method that uses circular Hough transform on an thresholded edge image of the retinal surface as in Barret et al. [15]. The Hough transform is able to find geometric objects in images by converting an object's equation into a Hough space parameter equation. For finding a circular objects as the optical disc we use:

$$(x_i - x)^2 + (y_i - y)^2 = r^2 \tag{1}$$

Although we use different a-priori values for the radius r of the optical disc it can be seen as a constrained parameter limiting the search for the optical disc to a two-dimensional problem. The Canny edge detection algorithm is used for generating the edge image. For most images the use of a fixed threshold within the canny edge detector leads to useful binary images. However with some images this fixed threshold yields too little or to many edges. To overcome this shortcoming a histogram of the magnitude image is created and only the highest five percent of the magnitude pixels are selected. Subsequently, the Hough transform to the edge map. Since a bigger circle contains more pixels resulting in an higher value in the accumulator matrix the accumulators are all normalized by multiplying with $1/\#circlepoints$. The accumulator cell with the highest value is chosen as the center of the optical disc (x, y).

However the method described sometimes yields poor results both in accuracy and detection time especially when testing robustness. In this case only few edges of the optical disc are detected making it often even impossible to locate it with the hough transform. Fig. 1 illustrates such a case.

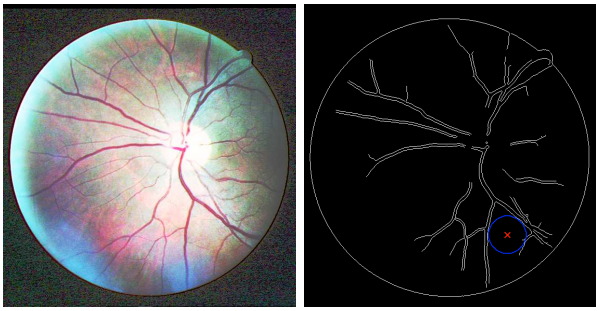

(a) Input image (b) Result

Fig. 1: Wrong optical disc location due to sparse edge map.

So we adapted the proposed method by not using an edge-based binary image as input for the Hough transform but taking into account the fact that the optical disc is usually an object with the highest luminance values. Another possible criterion suggested in literature is highest variance [16]. In order to use a global threshold t for all possible input images (and also distorted versions) we first apply a histogram equalization to the image. Using the highest 1 percent of the intensity image pixels ($t = 0.99$) a binary image is created that predominantly contains pixels of the optical disc. For finding the center of the circle that encloses these pixels finally the Hough transform is applied. Fig. 2 displays the steps for finding the optical disc. This method significantly improves results concerning accuracy. Detection speed was improved as well by a factor of 2.7 which is important for a fast user authentication. The reason for this improvement is that the range of admissible radii can be much more limited as compared to the first approach. As opposed to the first method where it was often impossible to detect the optical disc in histogram-equalized versions of the images the second method performs well in all robustness tests. Moreover the danger of the hough transform being fooled by detecting circles between edges resulting from vessels in sparse edge maps was removed.

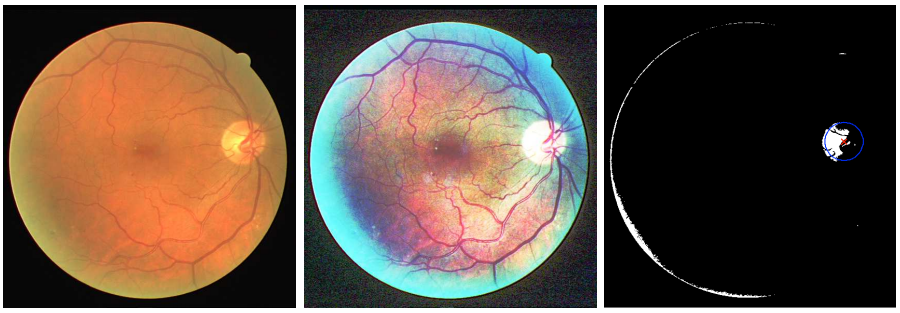

(a) Input image (b) Histogram Equal. (c) 1% brightest pixels

Fig. 2: Finding the optical disc

Consequently, we have used the second approach in our final experiments.

2.2 Vessel Extraction

Different approaches for automatic vessel segmentation have been proposed in literature (e.g. [7, 12]). We have chosen to adapt the MATLAB software package `mlvessel`[2] based on the wavelet-domain method described in [5] since it yields good results in enhancing vessel contrast while filtering out noise. First the retinal image is pre-processed by artificially extending the border that is defined by the camera's aperture in order to remove the strong contrast between the optical fundus and the image mask. Realizing that the wavelet transform is able to filter locally makes it effective for detecting local properties such as blood vessels. The continuous wavelet transform is defined

$$W_\psi(b, \Theta, a) = \frac{1}{\sqrt{a}} \int f(x)\psi^* \left(\frac{x-b}{a} \right) d^2x \tag{2}$$

with ψ^* denoting the complex conjugate of the 2-D Morlet wavelet ψ defined by [5] as:

$$\psi(x) = e^{ik_0 x} e^{-\frac{1}{2}|Ax|^2} \tag{3}$$

where $A = diag[\sqrt{\epsilon}, 1], \epsilon \geq 1$ is a 2 x 2 diagonal matrix defining the anisotropy of the filter. We only use the results produced by the Morlet wavelet with parameters $a = 2$, $k_0 = [0, 3]$ and $\epsilon = 4$ since this yields the best resolution of vessels. So for the scale value $a = 2$ maximum response over all possible angles Θ starting from 0 up to 170 degrees in steps of 10 is being calculated.

The resulting feature image is used for creating a binary vessel segmentation image by thresholding. Simple thresholding is the method of first choice because of its speed. However using a global threshold results in very different binary images concerning the number of vessels thus it is not very suitable for creating a retina template and matching. In order to achieve a well-balanced number of vessels in the binary images we first statistically determine the mean value of vessel pixels in a set of typical images suited for matching. For the data base used in our experiments (see Section 4.1) this gave us a mean value of vessel pixels of 8.5 % and a standard deviation of 1,5 %. Starting from a standard threshold of we slightly adjust the threshold up or down until the number of vessel pixels meets our above criteria. In order to get rid of unconnected vessels resulting from our thresholding process all connected objects that have fewer than a certain number of pixels are removed.

Fig. 3 shows the stages of the vessel extraction process. It is clearly visible that the stage of removing small pixel groups is strongly required (Fig. 3.b).

3 Retina Code Generation

Starting from the center of the optical disc we use concentric circles for taking samples from the binary vessel images. For construction of these circles we have

[2] `http://www.retina.iv.fapesp.br`

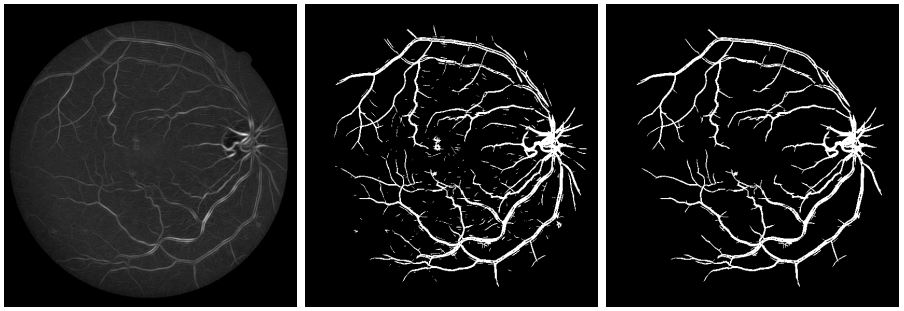

(a) Filtered image (b) Thresholding (c) Remove small objects

Fig. 3: Vessel Segmentation

implemented Bresenham's circle drawing algorithm [3]. For every circle pixel its value is set according to the underlying vessel or non-vessel pixel. Then the values of n_{avg} neighbouring circles are averaged and transformed to polar coordinates in steps of 1°. It is important to mention that outer circles usually degrade to circular arcs since the optical disc is mostly located at the left or right border of the retinal surface compare Fig. 4.c. This results in lower information density concerning the whole retina code which is further decreased by the higher arc length of the circles when using steps of 1° and the fact that the density of the vessels is usually higher around the optical disc. Thus hitting an underlying vessel pixel becomes more unlikely for bigger (outer) circles. This is conformed also in the example in Fig. 5.c. So we see that it is vital for our method to set the right parameters for the sampling procedure i.e. the number of samples (circles) N_{circ}, the averaging value n_{avg} (i.e. how many neighbouring circles are used for producing a single bit value), and the radius of the first circle r_0.

We investigate different retina code variants as shown in the settings of Table 1 in order to see how the sampling parameters affect the matching performance. The resulting retina codes are of sizes 360x5 (225 Byte), 360x10 (450 Byte) and 360x20 (900 Byte). These templates can be further compressed by using Run-Length Encoding since there are usually long sequences of non-vessel pixels within each code. Retica Systems Inc. provide the information of using 50-100 or even 20-50 bytes for their templates, but this could refer to encoded data.

Table 1: Sampling settings

Name	N_{circ}	n_{step}	n_{avg}	r_0
L1	15	3	3	5
L2	30	3	3	5
H1	60	5	3	5

Setting L1 only samples around the optical disc (only entire circles), L2 is the same as L1 but with increased N_{circ} and H1 also includes degraded circles. Fig. 4 shows examples of the samples taken for each setting.

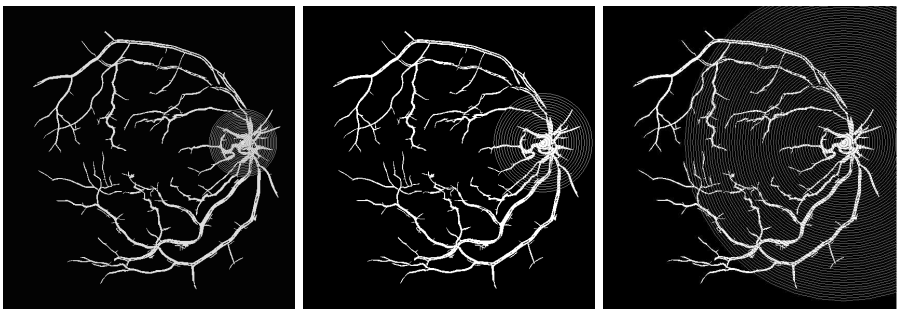

(a) Setting L1 (b) Setting L2 (c) Setting H1

Fig. 4: Sampling

Finally, the resulting retina codes from this sampling process are shown in Fig. 5.

(a) Setting L1

(b) Setting L2 (c) Setting H1

Fig. 5: Retina Codes

4 Experiments

4.1 Experimental Settings

We tested and evaluated our methods on a publicly available database of non-mydriatic images and corresponding manual vessel segmentations: the DRIVE[3] database [4]. The DRIVE database consists of 40 images that were captured in digital form from a Canon CR5 non-mydriatic 3CCD camera at 45 field of view (FOV). The images are stored in TIFF format of size 565 x 584 with 8 bits per color channel. Since the DRIVE database only contains images of different persons our experiments are limited to examining the inter person variability, FMR under image distortions, and different code sampling strategies. The green

[3] `www.isi.uu.nl/Research/Databases/DRIVE/`

channel of the non-mydriatic images shows the best contrast so we chose it for optical disc detection as well as for vessel extraction (and subsequent code generation). For the first optical disc detection technique, we use the Canny edge detector with parameters $\sigma = 1.0, t_{high} = 0.2, t_{low} = t_{high} \cdot 0.4$. Hough transform with various radii r ranging from 35 to 38 pixels is applied in the first approach, in the second approach we succeeded in using fixed radii around 36 pixels.

Matching between two distinct retina codes is done by calculating their Hamming Distance. In order to compensate for rotated versions of the images the two retina patterns are shifted against each other and the minimum of all Hamming distances is calculated. For each image to be tested the Hamming distance with each of the remaining templates in the database is determined ("leave one out" strategy). A pair having Hamming distance below a decision threshold T indicates a positive match.

For testing the robustness and the performance of our approach we generate several distorted versions of our input images by using the open-source tool `Imagemagick` (see Tab. 2 for the specifications) and matching the resulting templates with the images in the database.

Table 2: Robustness Tests

Test	Settings
JPEG	Quality 10%
JPEG2000	Compression ratio 100:1
Rotation	90°,−90° and 180°
Sharpening	r=1 pixel, σ=1, amount=500%
Hist. Equal.	Standard flat histogram

4.2 Experimental Results

The first step in testing our method is matching all retina codes against each other (for each of the settings shown in Tab.1) to see how the scores are distributed and if the codes are sufficiently discriminative. The mean relative Hamming distances $\bar{h}$, their standard deviations s_h, and the maximum and minimum Hamming distances h_{max} and h_{min} for this test are shown in Tab. 3. Assuming uncorrelated templates from different persons an average close to 0.5 in terms of Hamming distance is expected. In fact, the mean Hamming distances $\bar{h}$ are much smaller ($0.123 \leq \bar{h} \leq 0.216$). In addition to that, the range of obtained Hamming distances $[h_{min}, h_{max}]$ is very small and covers only 7-8% of the overall possible range.

Setting L2 shows the best results with respect to highest average Hamming distance values and standard deviation. The low values for H1 may be explained when taking Fig.5.c as example: of course, the large black areas – stemming from the circular arcs without any vessels close to the images' edges – in the code result in low Hamming distances. This is also true (in less pronounced

Table 3: Score distribution

	$\bar{h}$	s_h	h_{max}	h_{min}
L1	0.206	0.022	0.236	0.165
L2	0.216	0.028	0.250	0.172
H1	0.123	0.027	0.172	0.079

manner) for the other settings where we also find an imbalance between black (non-vessel) and white (vessel) areas causing low differences in general. These results indicate a very low inter personal variability of the generated code which makes the occurrence of false positive matches highly probable. While actual matching performance can not be derived directly from these values since intra personal variability can not be assessed at present state (due to the lack of corresponding data in the DRIVE database), low inter personal variability suggests the approach not to be suited for larger populations at least. The retina code example given by Retica Systems Inc. ("Multi-Radius Digital Pattern"[4]) seems to indicate even smaller potential for high variability (since the generation is not explained in detail, a reliable statement on this issue is not possible of course). Recall that Retica Systems Inc. claims a template size of 20 - 100 bytes whereas the smallest template investigated here has 225 byte. This of course worsens the situation for the commercial system. Also, the comparison to an iris code[5] suggests the retina code to be of significantly lower variability potential.

The results of the robustness test are shown in Tab. 4. Again, h_{max} denotes the highest relative Hamming distance of all matches, h_{min} the lowest value and FMR indicates the FMR ratio (ratio of false positive matches and the number of tests performed). The decision threshold T for computing FMR was derived from the score distribution test and is set to $T = h_{min}$ for all subsequent robustness and sampling tests (see Tab. 3).

Setting L2 performs best of all having only minor problems when the image is histogram-equalized. This is usually a problem with vessel segmentation yielding to many vessels and sometimes distorting the code too much. Both Settings L1 and L2 show very good robustness against false positive matches even under severe compression. This confirms previous results on lossy compression of biometric sample data not to effect FAR as long as applied in sensible ranges [17, 18]. Also rotation and sharpening does not lead to false positives in case of L2. A severe problem occurs with lowpass filtering. Here the vessels lying over the optical disc cannot be clearly distinguished any more, resulting in corrupted codes for all settings (since sampling near the optical disc is most crucial for our templates). Thus Lowpass filtering is omitted in Tab. 4. H1 shows very poor results with respect to robustness. Even rotation leads to 25% FMR although rotation is compensated in the matching stage. It is also remarkable that the higher sampling rate of H1 does not at all improve accuracy when using dis-

[4] `http://www.retica.com/site/images/howitworks.pdf`
[5] `http://www.retica.com/site/technology/irisretina.html`

torted images. Overall, it gets clear that the sampling strategy for H1 is not at all suited for generating sensible retina codes.

Table 4: Results of Robustness Tests

	L1			L2			H1		
	h_{max}	h_{min}	FMR	h_{max}	h_{min}	FMR	h_{max}	h_{min}	FMR
JPEG	0.115	0.053	0 %	0.107	0.064	0 %	0.074	0.032	0 %
JPEG2000	0.108	0.065	0 %	0.109	0.057	0 %	0.104	0.037	25 %
Rotation	0.151	0.073	0 %	0.115	0.081	0 %	0.095	0.039	25 %
Hist. Equal.	0.172	0.097	17.5 %	0.187	0.119	5 %	0.118	0.055	17.5 %
Sharpening	0.181	0.121	2.5 %	0.158	0.124	0 %	0.103	0.06	30 %

In order to see which template size is necessary for our method to achieve good results we further downsample the codes of all three settings to 180x5 (112.5 Byte) using nearest neighbour interpolation (see Tab. 5 for the results). Settings L1 and L2 performed quite well with JPEG, JPEG2000 and Rotation Tests. Hist. Equal. and Sharpening show an increased FMR between 10 and 35%. Setting H1 shows a major increase of FMRs which range from 5% with JPEG and JPEG2000 to a maximum of 90% with Hist. Equal. The high values of setting H1 probably results from a large code (360x20) being downsampled to 1/8 of the original size and thus loosing too much information.

Table 5: Results of Robustness Tests with downsampling

	L1			L2			H1		
	h_{max}	h_{min}	FMR	h_{max}	h_{min}	FMR	h_{max}	h_{min}	FMR
JPEG	0.124	0.044	0 %	0.126	0.065	0 %	0.095	0.037	5 %
JPEG2000	0.162	0.062	5 %	0.181	0.061	5 %	0.125	0.043	5 %
Rotation	0.081	0.031	0 %	0.092	0.035	0 %	0.112	0.057	10 %
Hist. Equal.	0.18	0.106	10 %	0.175	0.122	35 %	0.1	0.052	90 %
Sharpening	0.17	0.122	35 %	0.186	0.147	30 %	0.114	0.068	75 %

Considering the high compression rate JPEG2000 is operated with these results indicate that the code size could be actually reduced with respect to setting L2 for practical applications and still deliver acceptable results concerning compression robustness.

5 Conclusion and Future Work

We have discussed methods for generating retina codes from retinal images for biometric user authentication. The methods developed have exhibited very low inter personal variability – given the fact that retina based biometrics are probably restricted to high security environments due to the inconvenient data acquisition process, the real-life applicability of these techniques as a stand-alone

technique is as least questionable. It seems that the only sensible deployment could be in a multi-modal system in combination with iris recognition (as also offered by Retica Systems Inc.[6]) where the retina based part could perform an initial fast classification process identifying a set of possible matches in identification mode. For a final assessment intra personal variability has to be evaluated and related to FRR and FAR. Good robustness against JPEG and JPEG2000 compression not leading to false positives at low bitrates has been observed. Note that all those findings only apply to retina code templates but not for retina-scan based biometrics in general. For vessel-crossing based template data much better recognition performance has been reported.

Future work will involve a cooperation with the Department of Ophthalmology at the local hospital to get access to data allowing the determination of intra personal variability and to study the effects of eye diseases on a retina code based recognition scheme.

References

1. Gonzalez, R.C., Woods, R.E.: Digital Image Processing. Addison-Wesley Longman Publishing Co., Inc., Boston, MA, USA (2001)
2. ter Haar, F.: Automatic localization of the optic disc in digital colour images of the human retina. Master's thesis, Utrecht University (December 16 2005)
3. Bresenham, J.: A linear algorithm for incremental display of circular arcs. Communications of the ACM **20**(2) (February 1977) 100–106
4. Staal, J., Abramoff, M., Niemeijer, M., Viergever, M., van Ginneken, B.: Ridge based vessel segmentation in color images of the retina. IEEE Transactions on Medical Imaging **23**(4) (April 2004) 501–509
5. Soares, J.V.B., Leandro, J.J.G., Cesar-Jr., R.M., Jelinek, H.F., Cree, M.J.: Retinal vessel segmentation using the 2-d gabor wavelet and supervised classification. IEEE Transactions on Medical Imaging **25**(9) (September 2006) 1214–1222
6. Nanavati, S., Thieme, M., Nanavati, R.: Biometrics – Identity verification in a networked world. Wiley Computer Publishing (2002)
7. Leandro, J., Cesar, R., Jelinek, H.: Blood vessels segmentation in retina: Preliminary assessment of the mathematical morphology and of the wavelet transform techniques. In: Proc. Brazilian Symposium on Computer Graphics, Image Processing and Vision, (SIBGRAPI-01), Florianopolis, Brazil (2001) 84–90
8. Daugman, J.: How iris recognition works. IEEE Transactions on Circiuts and Systems for Video Technology **14**(1) (2004) 21–30
9. Ma, L., Tan, T., Wang, Y., Zhang, D.: Efficient iris recognition by characterizing key local variations. IEEE Transactions on Image Processing **13** (2004) 739–750
10. Ives, R., Guidry, A., Etter, D.: Iris recognition using histogram analysis. In: Conference Record of the 38th Asilomar Conference on Signals, Systems, and Computers. Volume 1., IEEE Signal Processing Society (November 2004) 562–566
11. Zhu, Y., Tan, T., Wang, Y.: Biometric personal identification based on iris patterns. In: Proceedings of the 15th International Conference on Pattern Recognition (ICPR'00). Volume 2., IEEE Computer Society (2000) 2801–2804

[6] `www.retica.com/site/technology/irisretina.html`

12. Vermeer, K., Vos, F., Lemij, H., Vossepoel, A.: A model based method for retinal blood vessel detection. Computers in Biology and Medicine **34** (2004) 209–219
13. Lin, T., Zheng, Y.: Node-matching-based pattern recognition method for retinal blood vessel images. Optical Engineering **42**(11) (2003) 3302–3306
14. Xu, Z., Guo, X., Hu, X., Chen, X., Wang, Z.: The identification and recognition based on point for blood vessel of ocular fundus. In: Proceedings of the 1st IAPR International Conference on Biometrics (ICB'06). Number 3832 in Lecture Notes on Computer Science (2006) 770–776
15. Barrett, S., Naess, E., Molvik, T.: Employing the hough transform to locate the optic disk. Biomedical Sciences Instrumentation **37** (2001) 86–81
16. Sinthanayothin, C., Boyce, J., Cook, H., Williamson, T.: Automated localisation of the optic disc, fovea, and retinal blood vessels from digital colour fundus images. British Journal of Ophthalmology **83** (1999) 902–910
17. Mascher-Kampfer, A., Stögner, H., Uhl, A.: Comparison of compression algorithms' impact on fingerprint and face recognition accuracy. In Chen, C., Schonfeld, D., Luo, J., eds.: Visual Communications and Image Processing 2007 (VCIP'07). Number 6508 in Proceedings of SPIE, San Jose, CA, USA, SPIE (January 2007) 650810–1 – 65050N–10
18. Rakshit, S., Monro, D.: Effects of sampling and compression on human iris verification. In: Proceedings of the IEEE International Conference on Acustics, Speech, and Signal Processing (ICASSP 2006), Tolouse, France (2006) II–337–II–340